A dynamic model of the type-2 inositol trisphosphate receptor

James Sneyd*† and Jean-François Dufour‡

*Institute of Information and Mathematical Sciences, Massey University, Albany Campus, Private Bag 102-904, North Shore Mail Centre, Auckland, New Zealand; and ‡Clinical Pharmacology, University of Bern, 35 Murtenstrasse, 3010 Bern, Switzerland

Edited by Charles S. Peskin, New York University, New York, NY, and approved November 27, 2001 (received for review June 5, 2001)

The dynamic properties of the inositol (1,4,5)-trisphosphate (IP_3) receptor are crucial for the control of intracellular Ca^{2+}, including the generation of Ca^{2+} oscillations and waves. However, many models of this receptor do not agree with recent experimental data on the dynamic responses of the receptor. We construct a model of the IP_3 receptor and fit the model to dynamic and steady-state experimental data from type-2 IP_3 receptors. Our results indicate that, (*i*) Ca^{2+} binds to the receptor using saturating, not mass-action, kinetics; (*ii*) Ca^{2+} decreases the rate of IP_3 binding while simultaneously *increasing* the steady-state sensitivity of the receptor to IP_3; (*iii*) the rate of Ca^{2+}-induced receptor activation increases with Ca^{2+} and is faster than Ca^{2+}-induced receptor inactivation; and (*iv*) IP_3 receptors are sequentially activated and inactivated by Ca^{2+} even when IP_3 is bound. Our results emphasize that measurement of steady-state properties alone is insufficient to characterize the functional properties of the receptor.

Oscillations and waves in the concentration of free intracellular calcium (Ca^{2+}) are seen in many cell types and are known to be an important intra- and intercellular signaling system. It is thus of interest to determine the mechanisms underlying such complex dynamic behavior. One of the most important of these mechanisms is the inositol trisphosphate receptor (IPR), which also functions as a Ca^{2+} channel. There is now a great deal of experimental evidence that in many cell types, oscillations and waves of Ca^{2+} are mediated in major part by the release through the IPR of Ca^{2+} from the endoplasmic reticulum, and that it is the modulation of the IPR by Ca^{2+} and by inositol (1,4,5)-trisphosphate (IP_3) that causes such complex dynamic behavior (1–7).

Models of the IPR thus play a central role in models of Ca^{2+} oscillations and waves, and a number of such models have been constructed (8–15). Most of them assume that the IPR can be modulated by the binding of Ca^{2+} and IP_3, and that Ca^{2+} plays a dual role, both activating and inactivating the IPR. However, recent experimental data are forcing us to reevaluate older models. One major problem with almost all older models of the IPR is that they assume that Ca^{2+} binds to the IPR with mass action kinetics, in which case the rate of IPR activation and inactivation increases approximately linearly with Ca^{2+} concentration ($[Ca^{2+}]$). However, experiments show that as $[Ca^{2+}]$ varies over five orders of magnitude, the rate of IPR inactivation varies over approximately only a single order of magnitude (16–18). This discrepancy can be avoided if we assume that each transition between receptor states is modulated by Ca^{2+} but is more complex than just simple Ca^{2+} binding by mass action kinetics.

Consider, for example, the reaction scheme shown in Fig. 1. If we assume that $\tilde{A}$ and $\bar{A}$ are in instantaneous equilibrium, we have $c\tilde{A} = L_1\bar{A}$, where $L_1 = l_{-1}/l_1$, and c denotes $[Ca^{2+}]$. Hence, letting $A = \bar{A} + \tilde{A}$, we have $dA/dt = (k_{-1} + l_{-2})I - \phi(c)A$, where $\phi(c) = c(k_1L_1+l_2)/c+L_1$. Thus, this scheme is a simple way in which saturating binding kinetics can be incorporated into a model. It is similar to the Michaelis–Menten model of an enzyme-catalyzed reaction, in which a saturating reaction rate is obtained by assuming the existence of an intermediate complex. In this introductory model, the state $\bar{A}$ plays a role similar to that of the enzyme complex. By assuming that the original state $\tilde{A}$ (analogous to the substrate) is in fast equilibrium with state $\bar{A}$, we attain saturating kinetics of the Michaelis–Menten type.

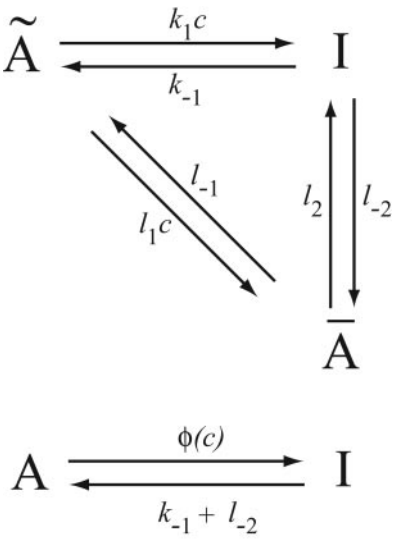

Fig. 1. Reaction diagram of a Ca^{2+}-dependent transition from state A to state I (c is Ca^{2+} concentration). If $\tilde{A}$ and $\bar{A}$ are in equilibrium, and if $A = \bar{A} + \tilde{A}$, then the upper reaction scheme is equivalent to the lower.

An IPR Model

A diagram of the IPR model is given in Fig. 2. Although it appears to contain a multiplicity of states, there are specific reasons for each one. The background structure is simple. Ignoring the various tildes, hats, and primes, we see that a receptor, R, can bind Ca^{2+} and inactivate to state I_1, or it can bind IP_3 and open to state O. State O can then shut (state S) or bind Ca^{2+} and activate to state A. State A can then bind Ca^{2+} and inactivate to state I_2. This structure is clearer in Fig. 3.

States $\bar{R}$, $\bar{O}$, $\bar{A}$, and R' are used to give Ca^{2+}-dependent transitions that have saturable kinetics, as in the simple example of Fig. 1. These states will ultimately disappear, leaving behind only functions of c. Note that the inactivated states I_1 and I_2 both have Ca^{2+} bound to the same site, but I_2

This paper was submitted directly (Track II) to the PNAS office.

Abbreviations: IP_3, inositol (1,4,5)-trisphosphate; IPR, IP_3 receptor.

†To whom reprint requests should be addressed. E-mail: j.sneyd@massey.ac.nz.

The publication costs of this article were defrayed in part by page charge payment. This article must therefore be hereby marked "*advertisement*" in accordance with 18 U.S.C. §1734 solely to indicate this fact.

www.pnas.org/cgi/doi/10.1073/pnas.032281999

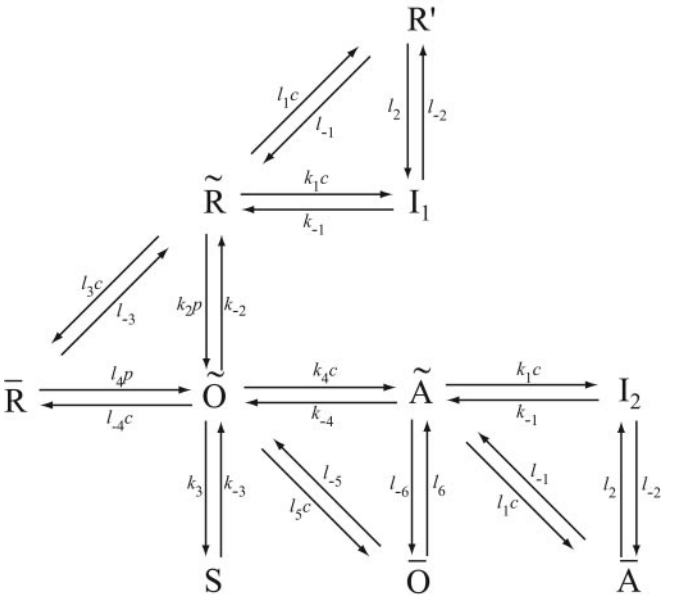

Fig. 2. The full IPR model. R, receptor; O, open; A, activated; S, shut; I, inactivated. c is $[Ca^{2+}]$; p is $[IP_3]$.

also has IP_3 and one other Ca^{2+} ion bound. For simplicity, we assume that the rate of Ca^{2+} binding to the inactivating site is independent of whether IP_3 is bound, or whether the receptor has been activated by Ca^{2+} (but see ref. 19 and later discussion). The $\tilde{R}$, $\bar{R}$, $\tilde{O}$ triangle models Ca^{2+}-dependent binding of IP_3; Ca^{2+} modulates the interconversion of the receptor between two states, each of which can bind IP_3 with different kinetics. In type-3 IPR, Ca^{2+} enhances IP_3 binding but inhibits IP_3 binding in type-1 IPR (20–22). The reaction scheme shown here incorporates either possibility, depending on the parameter values. As we shall see, our model predicts that Ca^{2+} increases the rate of IP_3 binding to type-2 IPR.

To derive the model equations, we first define $K_i = k_{-i}/k_i$ and $L_i = l_{-i}/l_i$ for every appropriate integer i. We also let c and p denote $[Ca^{2+}]$ and $[IP_3]$, respectively. Then, assuming that the transitions $\tilde{R} \rightleftarrows \bar{R}$, $\tilde{O} \rightleftarrows \bar{O}$, $\tilde{A} \rightleftarrows \bar{A}$ and $\tilde{R} \rightleftarrows R'$ are fast and in instantaneous equilibrium, we get $c\tilde{R} = L_3\bar{R}$, $c\tilde{R} = L_1R'$, $c\tilde{O} = L_5\bar{O}$, and $c\tilde{A} = L_1\bar{A}$. We now define the new variables $R = \bar{R} + \tilde{R} + R'$, $O = \bar{O} + \tilde{O}$, $A = \bar{A} + \tilde{A}$. Then

$$\frac{dR}{dt} = \phi_{-2}O - \phi_2pR + (k_{-1} + l_{-2})I_1 - \phi_1R,$$

$$\frac{dO}{dt} = \phi_2pR - (\phi_{-2} + \phi_4 + \phi_3)O + \phi_{-4}A + k_{-3}S,$$

$$\frac{dA}{dt} = \phi_4O - \phi_{-4}A - \phi_5A + (k_{-1} + l_{-2})I_2,$$

$$\frac{dI_1}{dt} = \phi_1R - (k_{-1} + l_{-2})I_1,$$

$$\frac{dI_2}{dt} = \phi_5A - (k_{-1} + l_{-2})I_2,$$

where

$$\phi_1(c) = \frac{(k_1L_1 + l_2)c}{L_1 + c(1 + L_1/L_3)},$$

$$\phi_2(c) = \frac{k_2L_3 + l_4c}{L_3 + c(1 + L_3/L_1)},$$

$$\phi_{-2}(c) = \frac{k_{-2} + l_{-4}c}{1 + c/L_5},$$

$$\phi_3(c) = \frac{k_3L_5}{L_5 + c},$$

$$\phi_4(c) = \frac{(k_4L_5 + l_6)c}{L_5 + c},$$

$$\phi_{-4}(c) = \frac{L_1(k_{-4} + l_{-6})}{L_1 + c},$$

$$\phi_5(c) = \frac{(k_1L_1 + l_2)c}{L_1 + c},$$

and where $R + O + A + S + I_1 + I_2 = 1$. Thus, given the fast equilibria above, Fig. 2 is equivalent to Fig. 3.

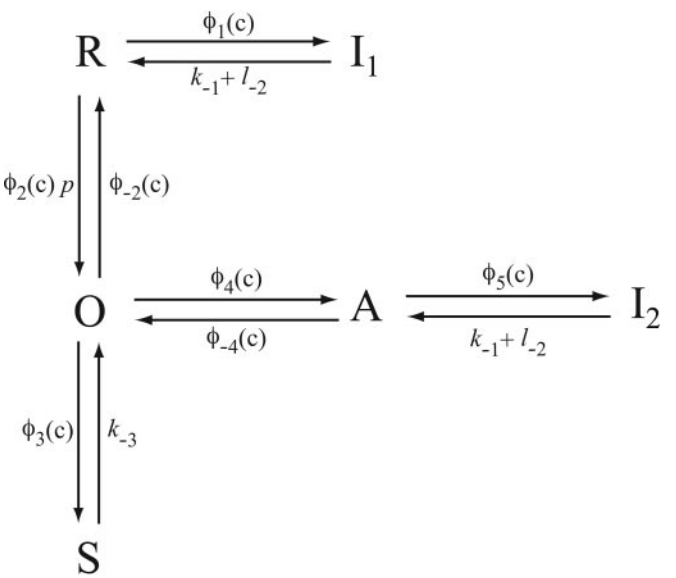

Fig. 3. Simplified diagram of the IPR model. Given the fast equilibria described in the text, this diagram is equivalent to that in Fig. 2.

The model assumes that the binding of IP_3 and Ca^{2+} is sequential, not independent. So, for instance, Ca^{2+} can bind to the activating site only after IP_3 has bound. Other models have made similar assumptions (10–12, 14) but without the correct dynamic behavior. Experimental data (23) indicate that the binding of IP_3 and Ca^{2+} are not independent events, with Ca^{2+} being unable to bind to the activating site until IP_3 has first bound.

There are three inactivated states; I_1, I_2, and S. States I_1 and I_2 have a Ca^{2+} bound to the same inactivating site, but I_2 also has IP_3 bound and Ca^{2+} bound to the activating site. State I_1 is necessary so that the receptor can inactivate in the absence of IP_3 (16). State I_2 is necessary so that an activated receptor may be inactivated by Ca^{2+}. State S is necessary so that an open receptor can inactivate in the absence of Ca^{2+} (18, 23).

We assume the IP_3 receptor consists of four independent and identical subunits and allows Ca^{2+} current when all four subunits are in state O, or all four are in state A, or some

PHYSIOLOGY

intermediate combination (for instance, when three are in state O, and one is in state A). Furthermore, we shall assume that the more subunits there are in state A, the greater the open probability of the receptor. With these assumptions, the open probability of the receptor is most conveniently written as $(0.1O + 0.9A)^4$. The numbers 0.1 and 0.9 are not crucial. Similar fits, essentially identical to visual inspection and with only small changes in parameter values, are obtained by using, for instance, $(0.1O + A)^4$ or $(0.05O + 0.9A)^4$ as the open probability (computations not shown). We note that the receptor must be able to pass Ca^{2+} current when all four subunits are in the O state, as it is known to allow Ca^{2+} current even in the absence of cytosolic Ca^{2+} (7).

The model closely follows the ideas of Taylor (7, 19, 23). Once IP_3 is bound, there is a competition between the intrinsic inactivation to state S and the Ca^{2+}-induced activation to state A. It is broadly consistent also with the scheme proposed by Hajnóczky and Thomas (24), in which the binding of IP_3 is modulated by Ca^{2+} binding, and binding of activating and inactivating Ca^{2+} happens sequentially. One difference between the model of ref. 24 and that presented here is that we assume that Ca^{2+} can bind directly to the inactivating site without first having to bind to the activating site. Another difference is that in ref. 24, the positive feedback action of Ca^{2+} on the receptor is mediated by the modulation of IP_3 binding alone, with no contribution from an activating binding site. Although our model includes the modulation of IP_3 binding by Ca^{2+}, the excitable nature of Ca^{2+} release results from the activation by Ca^{2+} (i.e., the O to A transition).

One major difference between our model and that of Taylor (19) is that we assume that an inactivating Ca^{2+} can bind even when IP_3 is already bound; i.e., the binding of IP_3 offers no protection to the inactivating site, as proposed in ref. 19. If, following Taylor, we assume the reverse, that Ca^{2+} cannot inactivate an IPR that already has IP_3 bound [i.e., we set $\phi_5(c) \equiv 0$], then we are unable to obtain acceptable fits to the dynamic data (computations not shown). Of course, we hasten to emphasize that this by no means rules out Taylor's hypothesis. We discuss this difference in more detail later.

Results and Discussion

The parameter values were determined by fitting the model to time courses of Ca^{2+} release from type-2 IPR at a fixed $[Ca^{2+}]$ and $[IP_3]$ (18) and to type-2 IPR steady-state data at a single $[IP_3]$ (25). For each time course (indexed by j), the net Ca^{2+} efflux (e_j) is measured at a sequence of time points, t_i. Dufour *et al.* (18) did not measure the receptor open probability directly but measured instead net Ca^{2+} release. This release will be proportional to the instantaneous open probability but with an unknown constant of proportionality. We made the simplest assumption, that this constant of proportionality is equal to one. To determine the objective function for each set of parameter values, we solved the differential equations (by using a forward Euler method with a time step of 0.001 s) to determine the model solution $m_j(t_i)$ at each of these time points and for each time course. The objective function corresponding to the time courses is then $\Sigma_{i,j}(e_j(t_i) - m_j(t_i))^2$.

In addition to the sum of squares shown above, the objective function included a sum of squares of differences between the model steady state and the data of (25) from type-2 IPR. The steady-state data of ref. 25 have open probabilities that reach as high as 0.5, a figure inconsistent with our dynamic data, because in the dynamic responses the open probabilities reached after the initial peak are approximately a factor of 10 smaller than the peak values. This difference is not possible if the steady-state open probability reaches as high as 0.5. However, there is extreme variation in the published open

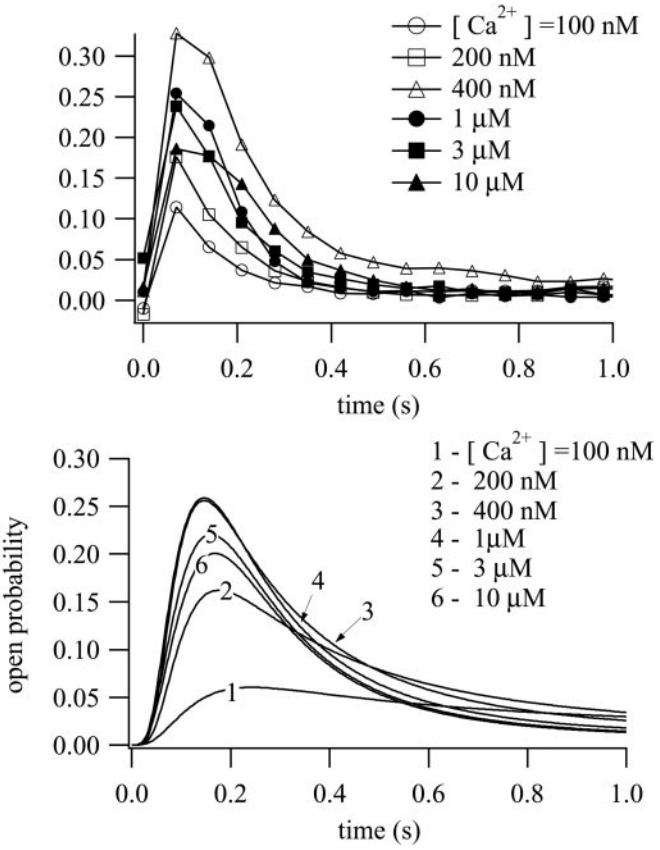

Fig. 4. (*Upper*) Data obtained from superfusion of $^{45}Ca^{2+}$-loaded hepatic microsomes. At $t = 0.10$ μM, IP_3 and the indicated $[Ca^{2+}]$ were added to the stimulus buffer and the Ca^{2+} flux measured as a function of time. Full details are given in ref. 18. (*Lower*) Ca^{2+} dose responses calculated from the model. Initial conditions were $R = 1$; all other receptor states were zero. At $t = 0$, 10 μM of IP_3 was added, with the indicated Ca^{2+} concentrations. Best-fit parameter values are: $k_1 = 0.64\ s^{-1}\cdot\mu M^{-1}$, $k_{-1} = 0.04\ s^{-1}$, $k_2 = 37.4\ s^{-1}\cdot\mu M^{-1}$, $k_{-2} = 1.4\ s^{-1}$, $k_3 = 0.11\ s^{-1}\cdot\mu M^{-1}$, $k_{-3} = 29.8\ s^{-1}$, $k_4 = 4\ s^{-1}\cdot\mu M^{-1}$, $k_{-4} = 0.54\ s^{-1}$, $L_1 = 0.12$ μM, $L_3 = 0.025$ μM, $L_5 = 54.7$ μM, $l_2 = 1.7\ s^{-1}$, $l_4 = 1.7\ s^{-1}\cdot\mu M^{-1}$, $l_6 = 4707\ s^{-1}$, $l_{-2} = 0.8\ s^{-1}$, $l_{-4} = 2.5$ $\mu M^{-1}\cdot s^{-1}$, and $l_{-6} = 11.4\ s^{-1}$.

probabilities of IPR, with peak values ranging from around 0.01 or less (27) to 0.5 or greater (25, 26, 28). The reasons for these differences are unclear. Thus, we chose to retain the qualitative nature of the type-2 IPR data of ref. 25 but to scale the data by a factor of 1/30 to force consistency with our dynamic data. We estimated the data of ref. 25 by eye from figure 7*B* (the curve labeled R-T2) of that paper.

A minimum of the objective function was then found by Powell's method (29). Typical parameters determined by the fit are shown in the caption to Fig. 4. The objective function was not sensitive to the precise parameter values. We also ensured that $K_1 = L_1L_2$, $K_2 = L_3L_4$, and $K_4 = L_5L_6$, so that the reaction scheme satisfies detailed balance.

Experimental and model Ca^{2+} dose responses are shown in Fig. 4. At $t = 0$, various concentrations of Ca^{2+} were added, all at $[IP_3] = 10$ μM. These time courses are faster than those in ref. 23 but agree well with those of refs. 16 and 19; the experiments of ref. 23 were in permeabilized cells, whereas those of refs. 16 and 18 were in microsome preparations, which may explain these differences. Another possible explanation of these differences is the different loading state of the stores. Our time courses agree well also with those of ref. 17; Parker *et al.* used *in vivo* pulses of IP_3 release in *Xenopus* oocytes to

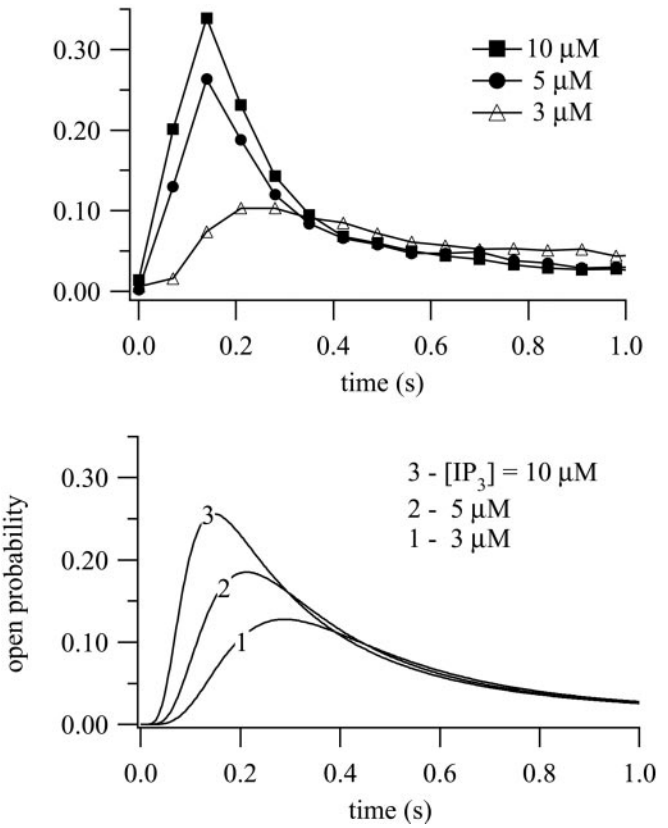

Fig. 5. (*Upper*) Data obtained from superfusion of $^{45}Ca^{2+}$-loaded hepatic microsomes. At $t = 00.4$ μM, Ca^{2+} and the indicated [IP_3] were added to the stimulus buffer and the Ca^{2+} flux measured as a function of time. Full details are given in ref. 18. (*Lower*) Model IP_3 dose responses. Initial conditions were $R = 1$; all other receptor states were zero (i.e., low Ca^{2+}, low IP_3). At $t = 00.4$, μM Ca^{2+} was added, together with the indicated [IP_3].

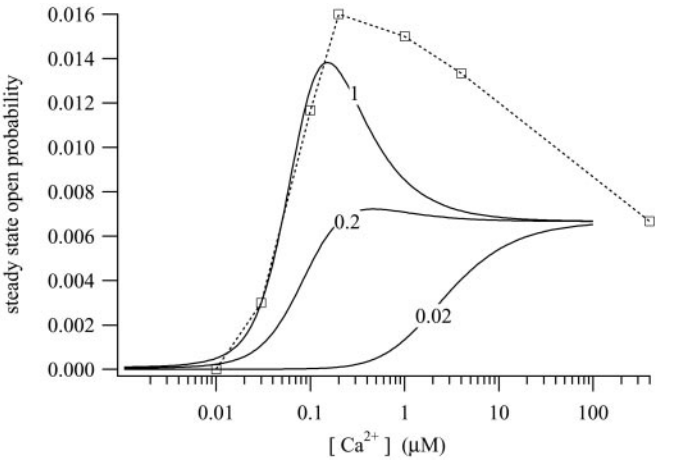

Fig. 6. Steady-state open probability of the IPR, measured at [IP_3] = 0.02, 0.2, and 1 μM. The symbols are the experimental data of ref. 25, from type-2 IPR, measured at [IP_3] = 1 μM. The data were estimated by eye from figure 7*B* of ref. 25.

measure the rate of Ca^{2+} release as a function of time, although not at constant [Ca^{2+}]. Experimental and model IP_3 dose responses are shown in Fig. 5. At $t = 0$, IP_3 was added at various concentrations, all at 0.4 μM Ca^{2+}. As [IP_3] increases, so does the response maximum. The model time courses show a clear latent period of around 20 ms before the open probability begins to rise, even at the highest [IP_3], similar to that seen experimentally (17, 30, 31).

The steady-state open probability of the model for various [IP_3] is shown in Fig. 6. At lower [IP_3], the steady-state curve is not bell-shaped, and at all [IP_3], the open probability remains nonzero as [Ca^{2+}] gets large.

Preincubation by Ca^{2+} or IP_3 attenuates the responses. After 0.3 s of exposure to 0.4 μM Ca^{2+}, in the absence of IP_3, the response maximum is greatly decreased (computations not shown), in agreement with ref. 16. Similarly, after 0.3 s of exposure to 1 μM IP_3, in the absence of Ca^{2+}, the response maximum is again greatly decreased (computations not shown). Although the time scales are different, this result is similar to the results of Marchant and Taylor (23).

In Fig. 7, we plot the various ϕ functions (note the different scale for ϕ_4). By comparing ϕ_2, ϕ_1, and ϕ_5, we see that the binding of IP_3 proceeds faster than the inactivation by Ca^{2+}. Activation by Ca^{2+} is much faster than either, with ϕ_4 being about an order of magnitude larger than all the other rate functions for all $c > 0.1$. This fast activation rate was a persistent feature of the fits and is consistent with previous modeling work (8, 9, 11, 14). Thus our model supports the theory that the dynamic responses are mediated by the fast activation and slower inactivation of the IPR by Ca^{2+}.

Our model predicts that Ca^{2+}-independent inactivation of the IPR by IP_3 has a time constant of around 10 s ($\phi_3 \approx 0.1$ s^{-1}), which is slower than the figure of 250 ms of ref. 23 but faster than the figure of 30 s of ref. 32. Our rate of Ca^{2+}-dependent IPR inactivation ($\phi_5 \approx 1.7$ at [Ca^{2+}] = 10 μM, giving a time constant of 588 ms) is slower than the figure of 50 ms of ref. 19 but is in excellent agreement with the figure of 580 ms (at 10 μM Ca^{2+}) of ref. 16. Our speed of the reversal of Ca^{2+}-induced IPR inactivation (around 800 ms) is slower than the figure of 400 ms of ref. 19. The rate of IP_3 dissociation from the IPR ($2 \leq \phi_{-2} \leq 7$, approximately, giving a time constant of 140–500 ms) agrees well with the figure of 450 ms of ref. 33, but the rate of IP_3 binding ($k_2 = 37.4$ $\mu M \cdot s^{-1}$) is slower than the figure of 120 $\mu M \cdot s^{-1}$ of ref. 33. Because of the different model structures, it is more difficult to compare our results to those of ref. 34; however, Moraru *et al.* get a Ca^{2+} binding on-rate of 10 $\mu M \cdot s^{-1}$, compared to our value of $k_4 = 4$ $\mu M \cdot s^{-1}$, and an IP_3 binding on-rate of 250 $\mu M \cdot s^{-1}$, compared to our value of $k_2 = 37.4$ $\mu M \cdot s^{-1}$. It thus appears that some of the rate constants predicted by our model lie within the experimentally observed ranges, whereas for others the deviations are greater. Differences in experimental method may account for some of these deviations, although it is highly likely that variability in the fitting procedure also plays an important role. The physiological effects of differences in the parameter values are even less clear. Not until such dynamic models are constructed for all the different receptor subtypes will we be able to study the functional importance of any differences in rate constants between receptor subtypes.

Because ϕ_2 is a decreasing function of c, the rate of IP_3 binding is decreased by higher [Ca^{2+}]. However, the steady-state [IP_3] for half-maximal binding can be calculated to be

$$\frac{F_2(k_{-1} + l_{-2} + \phi_1)}{(k_{-1} + l_{-2}(1 + F_4^{-1} + \phi_3/k_{-3}) + \phi_5 F_4^{-1}},$$

where $F_i = \phi_{-i}/\phi_i$. For the best-fit parameters, this equation is a decreasing function of c when $c > 0.1$ μM. Thus, when $c > 0.1$ μM, the steady-state sensitivity of the IPR to IP_3 increases as c increases, even though the rate of IP_3 binding decreases. Hence, *steady-state* measurements of the Ca^{2+} dependence of IP_3 bind-

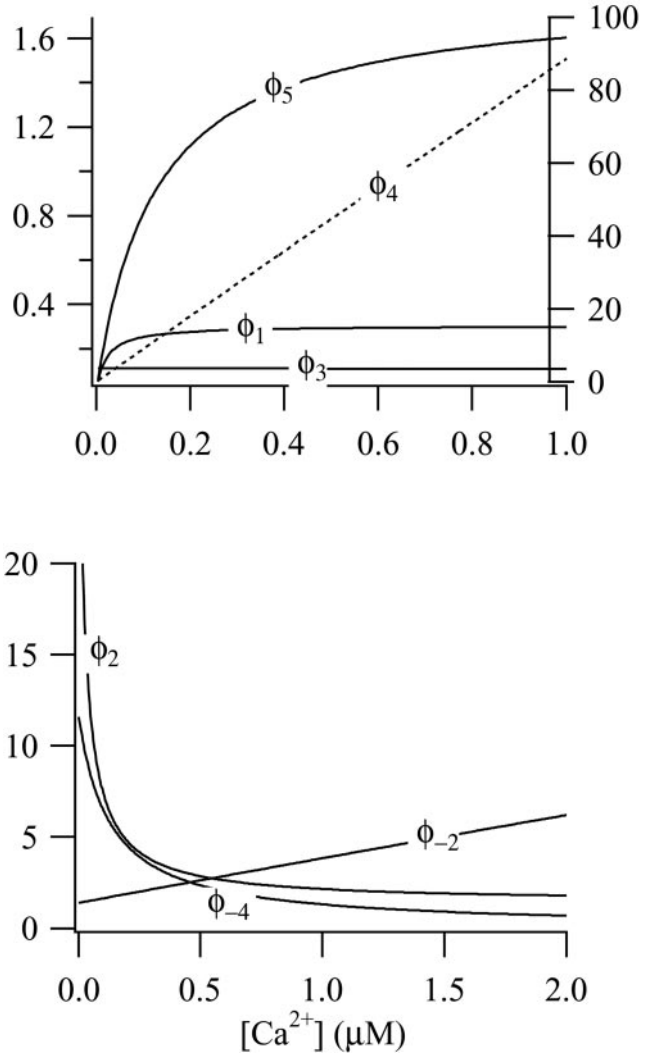

Fig. 7. The rate functions. The dotted curve, ϕ_4, is relative to the right-hand axis, whereas all the other curves are relative to the left-hand axis. All functions, except ϕ_2, are in units of s^{-1}. ϕ_2 has units of $\mu M^{-1} \cdot s^{-1}$.

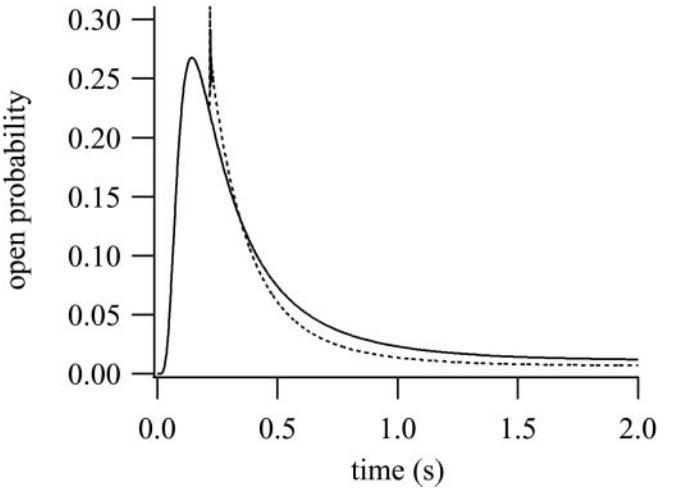

Fig. 8. The effect of the addition of high $[Ca^{2+}]$ after addition of IP_3. Solid curve: 10 μM IP_3 and 500 nM Ca^{2+} were added at $t = 0$. Dotted curve: same as the solid curve, except that at $t = 0.22$, 30 μM of Ca^{2+} was added.

ing give no information on the *dynamic* effects of Ca^{2+} on IP_3 binding.

It has been proposed that the binding of IP_3 renders the IPR unable to bind Ca^{2+} to the inactivating site (19), the evidence for this assertion being principally that the addition of a large concentration of Ca^{2+} does not inactivate the receptor once IP_3 is already bound. We simulate this experiment in Fig. 8. The solid line is the control response to the addition of 10 μM IP_3 and 500 nM Ca^{2+}. The dotted line is the result of adding (in addition to the control stimulation) 30 μM Ca^{2+} at $t = 0.22$. After the second addition of Ca^{2+}, the open probability initially rises as the receptor activates but then relaxes along much the same time course as the control response. The initial spike on the second addition of Ca^{2+} is very fast and unlikely to be easily detectable in superfusion studies. The results shown in Fig. 8 are qualitatively similar to those of ref. 19, even though our model assumes that Ca^{2+} can inactivate an IPR that has already bound IP_3. In addition, we investigated a model in which ϕ_5 was set to zero (i.e., modeling the assumption that the receptor cannot be inactivated by Ca^{2+} once it has bound IP_3). We were unable to obtain good fits of this model to the time-course data (computations not shown). Although this result does not imply that such a model cannot be made to fit the time-course data, in combination with the simulation of Fig. 8, it suggests that inactivation by Ca^{2+}, even when IP_3 is bound, is an important part of the response.

We conclude that, because of the saturating kinetics of Ca^{2+} activation and inactivation, the response to the addition of large amounts of Ca^{2+} may not be sufficient to determine whether the binding of IP_3 shields the Ca^{2+}-inactivating site.

J.S. was supported by the Marsden Fund of the Royal Society of New Zealand. J.-F.D. was supported by National Swiss Foundation Grant 3100-063696.00

1. Parker, I. & Ivorra, I. (1990) *Proc. Natl. Acad. Sci. USA* **87,** 260–264.
2. Yao, Y. & Parker, I. (1992) *J. Physiol.* **458,** 319–338.
3. Berridge, M. J. (1993) *Nature (London)* **361,** 315–325.
4. Sanderson, M. J., Charles, A. C., Boitano, S. & Dirksen, E. R. (1994) *Mol. Cell. Endocrinol.* **98,** 173–187.
5. Thomas, A. P., Bird, G. S. J., Hajnóczky, G., Robb-Gaspers, L. D. & Putney, J. W. J. (1996) *FASEB J.* **10,** 1505–1517.
6. Yoshida, Y. & Imai, S. (1997) *Jpn. J. Pharmacol.* **74,** 125–137.
7. Taylor, C. W. (1998) *Biochim. Biophys. Acta* **1436,** 19–33.
8. DeYoung, G. W. & Keizer, J. (1992) *Proc. Natl. Acad. Sci. USA* **89,** 9895–9899.
9. Atri, A., Amundson, J., Clapham, D. & Sneyd, J. (1993) *Biophys. J.* **65,** 1727–1739.
10. Othmer, H. & Tang, Y. (1993) *Experimental and Theoretical Advances in Biological Pattern Formation*, eds. Othmer, H., Murry, J. & Maini, P. (Plenum, London).
11. Bezprozvanny, I. (1994) *Cell Cal.* **16,** 151–166.
12. Tang, Y., Stephenson, J. L. & Othmer, H. J. (1996) *Biophys. J.* **70,** 246–263.
13. Laurent, M. & Claret, M. (1997) *J. Theor. Biol.* **186,** 307–326.
14. LeBeau, A. P., Yule, D. I., Groblewski, G. E. & Sneyd, J. (1999) *J. Gen. Physiol.* **113,** 851–871.
15. Sneyd, J., LeBeau, A. & Yule, D. (2000) *Physica D* **145,** 158–179.
16. Finch, E. A., Turner, T. J. & Goldin, S. M. (1991) *Science* **252,** 443–446.
17. Parker, I., Yao, Y. & Ilyin, V. (1996) *Biophys. J.* **70,** 222–237.
18. Dufour, J.-F., Arias, I. M. & Turner, T. J. (1997) *J. Biol. Chem.* **272,** 2675–2681.
19. Adkins, C. E. & Taylor, C. W. (1999) *Curr. Biol.* **9,** 1115–1118.
20. Yoneshima, H., Miyawaki, A., Michikawa, T., Furuichi, T. & Mikoshiba, K. (1997) *Biochem. J.* **322,** 591–596.
21. Cardy, T. J., Traynor, D. & Taylor, C. W. (1997) *Biochem. J.* **328,** 785–793.
22. Sienaert, I., Missiaen, L., De Smedt, H., Parys, J. B., Sipma, H. & Casteels, R. (1997) *J. Biol. Chem.* **272,** 25899–25906.
23. Marchant, J. S. & Taylor, C. W. (1998) *Biochemistry* **37,** 11524–11533.
24. Hajnóczky, G. & Thomas, A. F. (1997) *EMBO J.* **16,** 3533–3543.

25. Ramos-Franco, J., Bare, D., Caenepeel, S., Nani, A., Fill, M. & Mignery, G. (2000) *Biophys. J.* **79,** 1388–1399.
26. Mak, D.-O. D., McBride, S. & Foskett, J. K. (2001) *J. Gen. Physiol.* **117,** 435–446.
27. Kaftan, E. J., Ehrlich, B. E. & Watras, J. (1997) *J. Gen. Physiol.* **110,** 529–538.
28. Mak, D.-O. D., McBride, S. & Foskett, J. K. (1998) *Proc. Natl. Acad. Sci. USA* **95,** 15821–15825.
29. Press, W. H., Teukolsky, S. A., Vetterling, W. T. & Flannery, B. P. (1992) *Numerical Recipes in Fortran* (Cambridge Univ. Press, Cambridge, U.K.), 2nd Ed.
30. Marchant, J. S. & Taylor, C. W. (1997) *Curr. Biol.* **7,** 510–518.
31. Ogden, D. & Capiod, T. (1997) *J. Gen. Physiol.* **109,** 741–756.
32. Mak, D.-O. D. & Foskett, J. K. (1997) *J. Gen. Physiol.* **109,** 571–587.
33. Meyer, T., Wensel, T. & Stryer, L. (1990) *Biochemistry* **29,** 32–37.
34. Moraru, I. I., Kaftan, E. J., Ehrlich, B. E. & Watras, J. (1999) *J. Gen. Physiol.* **113,** 837–849.